ORIGINAL PAPER

physica status solidi b

www.pss-b.com

Check for updates

High-Quality Si-Doped β-Ga_2O_3 Films on Sapphire Fabricated by Pulsed Laser Deposition

*Sergiy Khartsev, Nils Nordell, Mattias Hammar, Juris Purans, and Anders Hallén**

Pulsed laser ablation is used to form high-quality silicon-doped β-Ga_2O_3 films on sapphire by alternatively depositing Ga_2O_3 and Si from two separate sources. X-ray analysis reveals a single crystallinity with a full width at half maximum for the rocking curve around the (−201) reflection peak of 1.6°. Silicon doping concentration is determined by elastic recoil detection analysis (ERDA), and the best electrical performance is reached at a Si concentration of about 1×10^{20} cm^{-3}, using optimized deposition parameters. It is found that a high crystalline quality and a mobility of about 2.9 cm^2 $(V\,s)^{-1}$ can be achieved by depositing Si and Ga_2O_3 from two separate sources. Two types of Schottky contacts are fabricated: one with a pure Pt and one with a PtO_x composition. Electrical results from these structures are also presented.

1. Introduction

The wide bandgap semiconductor Ga_2O_3 has over the last 5 years become one of the most investigated and reported materials. One major reason for this exploding interest is the potential applications of, particularly, the β-Ga_2O_3 polymorph as high voltage electric power rectifiers and switches. The possibility to fabricate inexpensive substrate wafers directly from melt, in addition to the extremely high breakdown capabilities demonstrated for this material, gives a competitive edge over other wide bandgap materials, such as SiC and GaN.[1,2] Pulsed laser deposition (PLD) is a technique based on physical vapor deposition, where powerful laser pulses are used to vaporize a target that subsequently deposits on a substrate. Using a proper combination of pressure, ambient gases, and temperature, species from the ablated material condense on the substrate and form a homogeneous thin film that may also grow epitaxially. While the physical mechanisms involved are highly complex and to some extent unknown, the technique has proven practically useful in many applications. In this contribution, we demonstrate PLD of high-quality β-Ga_2O_3 films and that it is also possible to control the inclusion of n-type dopants, i.e., silicon, in the process by alternatively depositing Si and Ga_2O_3 from two separate sources. PLD of Ga_2O_3 has been demonstrated previously and most of these early references primarily investigate the material quality of β-Ga_2O_3 deposited on Al_2O_3.[3–6] Later, pulsed laser deposited β-Ga_2O_3 on Al_2O_3 has also been used for demonstrating device applications, such as solar-blind UV detectors[7,8] and Schottky diodes, for instance, with Cu,[9] Ni,[10] and Ir[11] contacts. Silicon, a common impurity in Ga_2O_3 grown from melt, has been shown to be acting as a donor and contribute to the n-type character of substrates, presumably residing on substitutional Ga sites.[12] While most previous PLD-deposited Si-doped Ga_2O_3 has used a silicon-doped target for the PLD process,[13] in this article the Si doping is controlled by shifting the target during deposition from a nominally undoped Ga_2O_3 target to a pure Si target. By shifting the target to Si every 50th pulse (1 out of 50 pulses) during a run, a Si doping of about 1 at% is achieved. This layer works as a conductive backside onto which a second (unintentionally) low-doped layer is grown by ablating only from the Ga_2O_3 target. Platinum and Pt oxide are then evaporated on the low-doped layer to form Schottky barriers, whereas the backside obtains Ohmic contacts. (For details see the Experimental Section.) Structural characterization of the produced material and electrical characterization of the diodes are presented. It is shown that the technique with PLD from dual sources is able to yield high-quality β-Ga_2O_3 with a good control of the Si doping.

Dr. S. Khartsev, Dr. N. Nordell, Prof. M. Hammar, Prof. A. Hallén
School of EECS
Royal Institute of Technology KTH
P.O. Box Electrum 229, Kista-Stockholm SE 164 40, Sweden
E-mail: ahallen@kth.se

Prof. J. Purans
Institute of Solid State Physics ISSP
Kengaraga Street 8, Riga LV-1063, Latvia

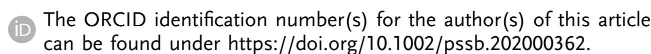
The ORCID identification number(s) for the author(s) of this article can be found under https://doi.org/10.1002/pssb.202000362.

© 2020 The Authors. Published by Wiley-VCH GmbH. This is an open access article under the terms of the Creative Commons Attribution-NonCommercial License, which permits use, distribution and reproduction in any medium, provided the original work is properly cited and is not used for commercial purposes.

DOI: 10.1002/pssb.202000362

2. Results and Discussion

Results from X-ray diffraction (XRD) are shown in **Figure 1**. This Si-doped β-Ga_2O_3 reference film is about 440 nm thick and the (−201), (−402), and (−603) peaks are seen, indicating well (−201)-oriented, single-phase film. The rocking curve around the (−201) reflection peak displays a full width at half maximum of 1.6°, which compares well with β-Ga_2O_3 of standard quality on *c*-cut sapphire.[14–16]

Optical transmittance in the wavelength range from 200 to 800 nm is shown in **Figure 2**. The spectrum is from only the

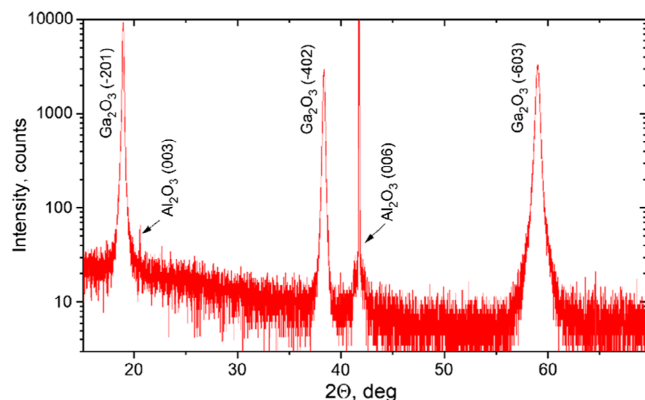

Figure 1. XRD spectrum from Θ–2Θ scan, using Cu Kα radiation of a Si-doped β-Ga_2O_3 440 nm reference film gown on (0001) Al_2O_3 single crystal (*c*-cut sapphire).

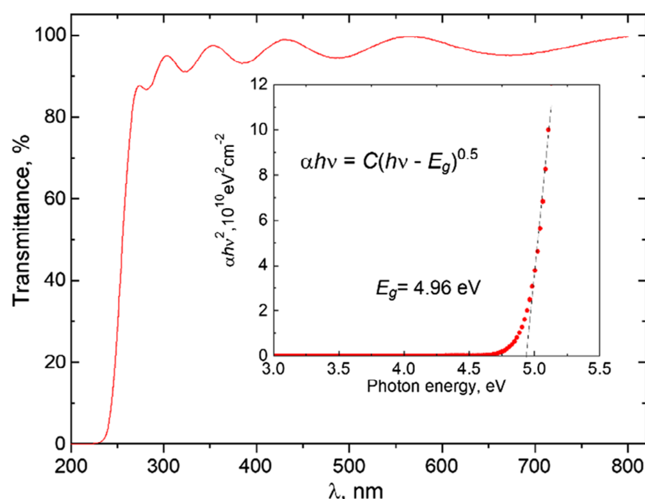

Figure 2. UV–vis transmittance for the 440 nm Si:Ga_2O_3 film, normalized by the transmittance from the sapphire substrate. The inset shows the Tauc plot for evaluation of the bandgap ($E_g = 4.96$ eV).

440 nm Si:β-Ga_2O_3, where the signal from the sapphire substrate has been used as reference. A bandgap of 4.96 eV is deduced from the Tauc plot,[17] which is well in agreement with published values for the β-Ga_2O_3 bandgap.

Figure 3 shows ion beam analysis of the elemental content in the film. The method used is elastic recoil detection analysis (ERDA), where heavy, high energy ions, 37 MeV ^{127}I, are used as a primary beam to eject secondary ions from the film. In the ERDA measurement, the energy of recoiling target ions is detected both with a time-of-flight detector and a conventional silicon surface barrier detector. By plotting the energy versus flight time, it is possible to separate the contribution to the spectrum from different masses because for a low mass and a high mass ion with the same energy the flight time will be longer for the heavier element. In contrast to the more common ion beam analysis technique Rutherford backscattering spectrometry (RBS), ERDA also enables in this way detection of lighter elements in a film with heavier atoms. It would, for instance,

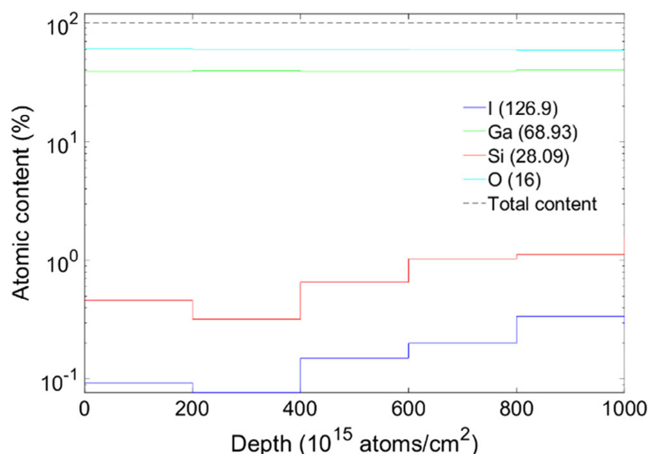

Figure 3. Data from elastic recoil detection analysis, ERDA, using 37 MeV ^{127}I as incident ions from the highly Si-doped β-Ga_2O_3 layer. The depth scale is expressed in units of 10^{15} atoms cm^{-2}, where 300×10^{15} atoms cm^{-2} correspond to about 100 nm. Also, note that the concentration values are mean values estimated for broad "slices" of the sample, giving a nonphysical step-like appearance of the elemental concentration.

not be possible to detect Si in our samples with RBS because backscattering from the much heavier and more abundant Ga atoms would totally dominate an RBS spectrum. The concentration of various elements in the film deduced from the ERDA measurements is shown in Figure 3 as a function of the depth from the sample surface.

From the plot we see that stoichiometric ratio between Ga and O (40% Ga and 60% O) is maintained throughout the film. A problem with estimating the atomic abundance of trace elements is that the surface region most often is contaminated, for instance, by water and hydrocarbons. This makes it difficult to obtain reliable concentration values closer to the surface for lower concentrations because the method used for the calculation requires that the total sum of the different elements must add up to 100%. This may be the reason for a slightly lower Si concentration closer to the surface, but according to the ERDA measurements, the Si concentration lies in the range of 0.4–1 at% in the film. This corresponds to a Si concentration of about 2×10^{20} cm^{-3}. From Hall measurements at room temperature on the same films (not shown), a carrier density of about 2.5×10^{19} cm^{-3} is found, which is slightly less than a factor of 10 lower than the Si content measured by ERDA. This could indicate that not all Si atoms are active and contribute to the free carrier concentration. One can speculate that the Si deposited by the single pulses on the pure Si target produces delta-doped sub-nm thick layers of high Si concentration, separated by 3–4 nm of Ga_2O_3. However, diffusion of Si should occur and spread the donor to the unintentionally doped regions between the delta-doped layers. This diffusion is expected, particularly because the PLD is done under oxygen ambient, which is known to enhance defect-assisted diffusion of Si via Ga substitutional sites.[18] Nevertheless, it seems that most of the Si is present as nonactivated impurities, perhaps forming Si precipitates, or SiO_2. One can also note that in Figure 3 also a signal from

 © 2020 The Authors. Published by Wiley-VCH GmbH

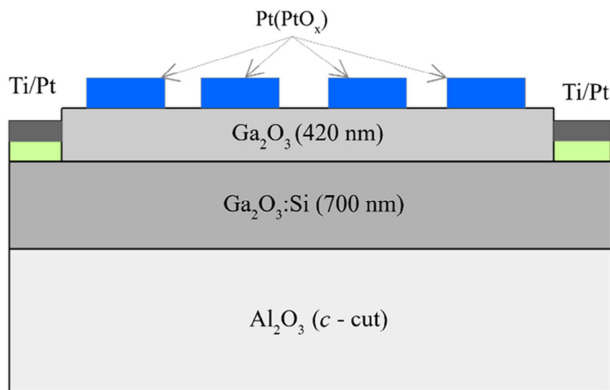

Figure 4. Schematic of the fabricated diode structures. From bottom, Al_2O_3-substrate wafer, Si-doped β-Ga_2O_3 with thickness 700 nm, nominally undoped β-Ga_2O_3 with thickness 420 nm, circular Pt or PtO_x contact pads with diameter of 0.5 mm. Along the sides of the structure Ti/Pt stripes are deposited on the highly conductive Si-doped β-Ga_2O_3 layer.

the primary ions, iodine, can be seen. This signal will increase as the measurement proceeds. As a final remark regarding the Hall measurements, it should be mentioned that the measurements gave an electron mobility of 2.9 cm^2 $(V\,s)^{-1}$, which compares well with other studies of PLD-produced β-Ga_2O_3.[19] The resulting conductivity is 11.7 S cm^{-1} and ensures that the Si-doped layer will function as a low resistive backside contact.

Figure 4 shows a schematic cross section of the Schottky diodes that are fabricated on top of the Si-doped Ga_2O_3 film. Two varieties of contacts are attempted: deposition of plain Pt and deposition of PtO_x. Thin oxide layers have recently been used to tailor the barrier height and also improve thermal and mechanical properties of the contacts.[20] In **Figure 5**, the results from capacitance–voltage measurements of the two types of Schottky structures at room temperature are shown, plotted as $1/C^2$ versus voltage. From the slopes, a homogeneous doping

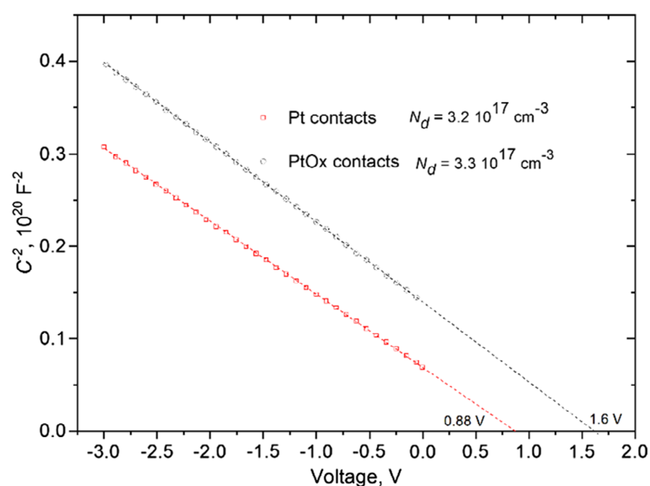

Figure 5. Capacitance–voltage measurements, plotted as $C^{-2}(V)$, of the Pt/Ga_2O_3 and PtO_x/Ga_2O_3 structures, showing a very homogeneous net doping concentration of 3.2 and 3.3 × 10^{17} cm^{-3} for the two samples. The intercept with the x-axis is also indicated. The capacitance is measured at room temperature and 100 kHz.

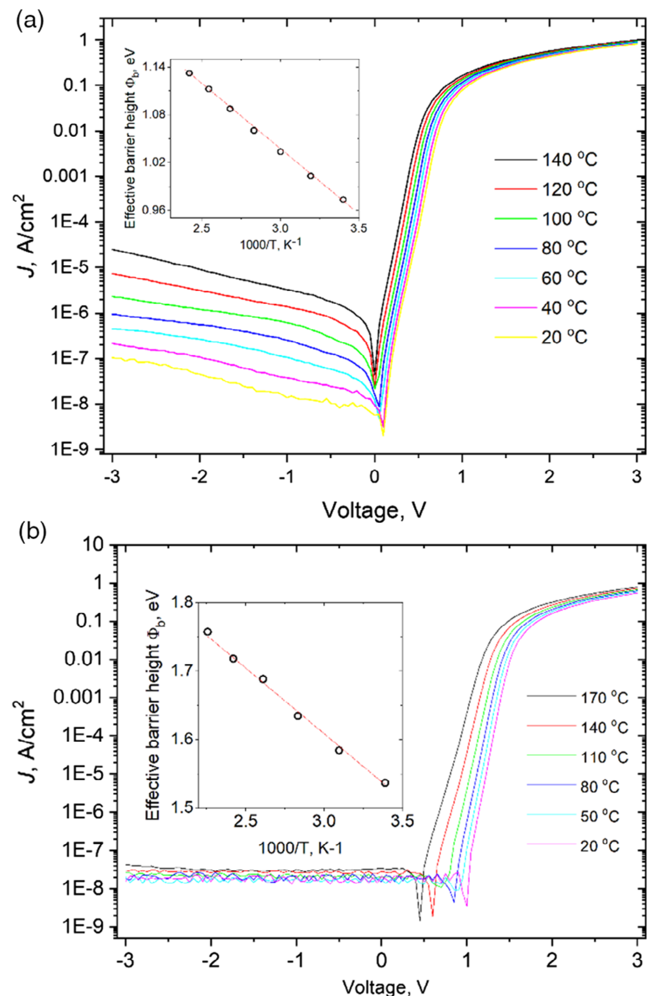

Figure 6. Current–voltage characteristics for a) the Pt/Ga_2O_3 and b) PtO_x/Ga_2O_3 for various temperatures in the range of 20–140 and 20–170 °C, respectively. The inset shows the effective barrier height versus the inverse temperature.

of 3.2 and 3.3 × 10^{17} cm^{-3} is obtained for the Pt/Ga_2O_3 and the PtO_x/Ga_2O_3 contacts, respectively. From the intercept with the x-axis, the PtO_x contact displays nearly doubled built-in potential compared with the plain Pt, 1.6 and 0.9 V for the PtO_x and the Pt contacts, respectively.

Figure 6a,b shows the current density versus voltage (J–V) characteristics under forward and reverse bias for the Pt/Ga_2O_3 and PtO_x/Ga_2O_3 structures, respectively, for various temperatures. A rectifying ratio of about seven to eight orders of magnitude can be seen at room temperature. In the inset, the effective barrier heights, Φ_B, are deduced as a function of the inverse temperature.

Although no sophisticated analysis of the J–V characteristics has been done at this point, it is clear that the oxidized contact (Figure 6b) has a clearly larger barrier and that the leakage current under reverse bias is kept well below 10^{-7} A cm^{-2}, even at temperatures above 170 °C. The values on effective barrier height from C–V measurements appear to be very similar to what was obtained for the Pt/Ga_2O_3 contact (0.90 eV),[20] but lower than the

© 2020 The Authors. Published by Wiley-VCH GmbH

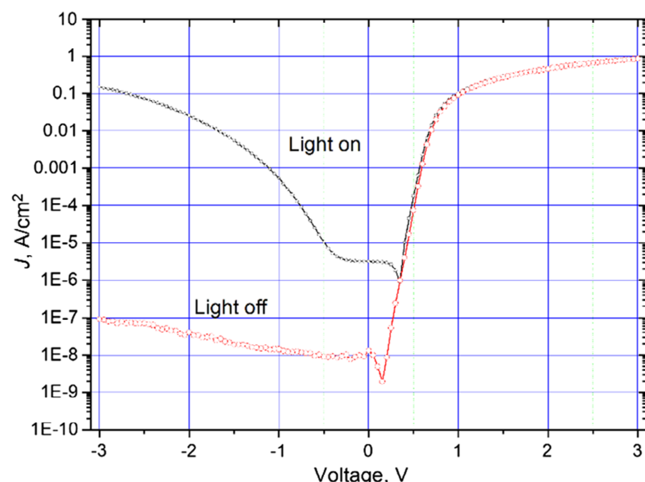

Figure 7. Room temperature current–voltage characteristics for the Pt/Ga_2O_3 structure with and without illumination with 360 nm light.

same reference regarding the oxidized PtO_x/Ga_2O_3 contact (1.97 eV). Hou et al.[20] explained the increased barrier height, improved rectifying performance, and better thermal stability for the oxidized contact with passivation of oxygen vacancies close to the interface, as well as significant increase in work function. On the contrary, He et al.[21] indicated for a pure Pt contact on edge-defined film-fed grown β-Ga_2O_3 films a value of the built-in potential of 1.16 V, i.e., higher than what is reported here. These discrepancies indicate the difficulties to compare electrical measurements because the behavior of the metal–semiconductor contact is so strongly dependent on the fabrication procedures and the surface properties.

Figure 7 shows the J–V characteristics of the Schottky diode with Pt contact at room temperature again, but this time also under illumination with a 360 nm LED. The behavior of the PtO_x contact is similar, but less pronounced. Apparently, the material contains self-trapped carriers that are excited by this light of an energy slightly below the bandgap. The current relaxation process, when the light is turned off, fits well to a two-exponent decay equation with a slow ($\tau_1 = 50.63$ s) and a fast ($\tau_2 = 3.26$ s) component. These relaxation times are in excellent agreement with those reported by Guo et al.[22] for 365 nm illumination ($\tau_1 = 51.26$ s and $\tau_2 = 3.46$ s, while for 254 nm the response is approximately 3 times faster: $\tau_1 = 16.61$ s and $\tau_2 = 1.02$ s). Even if we expect our device to be 3 times faster for the UVC range (200–280 nm), it remains extremely slow compared, for example, with Ga_2O_3/p-type 4H-SiC deep UV photodiode with 30 μs rise/fall time.[23] Improvement of dynamic characteristics of our structure demands better control of the growth process to reduce defects and impurities, to avoid the trapping effect.

3. Conclusion

Pure Pt and oxidized Pt Schottky diodes are fabricated by PLD of (−201)-oriented β-Ga_2O_3 on a sapphire substrate. A Si-doped β-Ga_2O_3 layer functions as a backside contact, where a separate Si target is ablated by every 50th pulse to give a doping concentration in the order of 1 at%. A nominally undoped β-Ga_2O_3 layer is then deposited and the two types of Pt contacts are formed on top of this structure. X-ray measurements indicate a single-phase well-oriented material along the (−201) direction, whereas Hall measurements of the Si-doped layer give a mobility of 2.9 $cm^2 (V s)^{-1}$ and a free carrier concentration of 2.5×10^{19} cm^{-3}. Comparing the number of free carriers with chemical content of Si using ERDA, it means that 10–20% of the Si atoms is activated. The Schottky diodes also perform well with a rectification ratio of about eight orders of magnitude. The oxidized Pt contacts show a larger barrier and a much lower leakage current under reverse bias, compared with pure Pt contacts. In conclusion, the investigation shows that it is possible to use PLD at 600 °C, and achieve high-quality β-Ga_2O_3 and also control the doping by a second Si target, to fabricate Schottky structures on an insulating substrate. However, there are still many optically active defects present in the material and more work is needed to reduce impurities and dislocation density, as well as understanding the role of Pt/Ga_2O_3.

4. Experimental Section

Highly Si-doped β-Ga_2O_3 films were prepared on (0001) Al_2O_3 substrates using PLD technique. Unlike commonly used ablation of preliminary Si-doped Ga_2O_3 targets, we used an alternative ablation procedure of using one pure Ga_2O_3 target and one high purity Si target to ensure a flexibility in the optimization of Si content needed for high conductivity and mobility of the films. Prior to deposition, (0001) Al_2O_3 substrates ($7 \times 7 \times 0.5$ mm^3) were sequentially sonicated in acetone, ethanol alcohol, and deionized water and purged by nitrogen. An excimer laser, CompPex 110 (248 nm, 30 ns), was used to ablate ceramic Ga_2O_3 of 90% density and 99.99% purity (diameter 25 mm) and high purity silicon wafer (diameter 55 mm). Targets were rotated/rastered to avoid nonuniform wearing and related problems. The optimal conditions for the deposition were 600 °C substrate temperature and 3 mTorr of argon/oxygen (95:5) mixture background pressure. The partial pressure of oxygen was a critical parameter, but the presence of Ar helped to keep the chamber's laser port free from deposits during processing, thus providing constant energy delivered to the targets. At these conditions—a laser fluency of 2.5 J cm^{-2} and 50 mm substrate-to-substrate distance—the deposition rate was around 0.7 Å $shot^{-1}$. Depositions were performed at laser repetition rate of 4 Hz. We took special measures for stable and droplet-free ablation of the silicon target. Due to a rapid Si surface modification induced by the laser radiation (for the given wavelength and pulse duration), deposition rate drastically changed with increased number of pulses per site and became more or less stable only after a certain preablation treatment. Unfortunately, further target exposition soon caused the appearance of micron-sized droplets on the film surface. Such defects were extremely undesirable for the multilayered diode structure because the droplets might work as a source of leakage current, or even led to short-circuit failure in the diodes. Here, we used a large Si target, freshly ground and identically preablated, for each deposition run. Apart from that, during the deposition the position of the target was changed in such a way as to expose a "fresh" site for each Ga_2O_3–Si layer, ensuring a stable silicon yield per shot and droplet-free film surface.

An array of Ga_2O_3 Schottky diodes was fabricated using the optimized deposition conditions and a Si concentration corresponding to a 50:1 ratio of laser shots was applied to Ga_2O_3 and Si targets, respectively, forming a highly Si-doped Ga_2O_3 bottom layer, 700 nm thick, serving as a conductive template. A nominally undoped gallium oxide film was then deposited by ablating only from the Ga_2O_3 target, and to finalize the stack, Pt Schottky contacts, diameter of 0.5 and 100 nm thick, were radio frequency magnetron sputtered on the top of upper layer, using Ar atmosphere. Also, deposition of PtO_x was tried, using an ambient of 4:10 O_2/Ar mixture. Two Ti/Pt (100/100 nm) stripes deposited at the edges of the Si-doped

© 2020 The Authors. Published by Wiley-VCH GmbH

template and masked during the deposition of undoped Ga_2O_3 layer were used as ohmic contacts.

Regarding characterization, the X-ray measurements were performed with Empyrean XRD system (PANalytical) with Cu Kα source. The Si concentration was established by heavy ion ERDA, using 37 MeV ^{127}I ions as the primary beam. A Tencor P-15 profilometer was used to determine film thickness and surface roughness, which was found to be as low as 2–3 nm for a 500 nm-thick Ga_2O_3 film. Electrical characterization was performed using a Keithley 2002 multimeter, a Keithley 6517A electrometer, and a Philips PM6304 LCR-meter.

Acknowledgements

The EU Horizon 2020 project CAMART^2 is acknowledged for partly supporting the project, and the Ion Technology Centre, ITC, in Sweden is acknowledged for ion beam analysis (ERDA).

Conflict of Interest

The authors declare no conflict of interest.

Keywords

diodes, fabrication, gallium oxide, pulsed laser deposition, wide bandgap

Received: July 2, 2020
Revised: August 18, 2020
Published online:

[1] M. Higashiwaki, G. H. Jessen, *Appl. Phys. Lett.* **2018**, *112*, 060401.
[2] S. J. Pearton, F. Ren, M. Tadjer, J. Kim, *J. Appl. Phys.* **2018**, *124*, 220901.
[3] M. Orita, H. Hiramatsu, H. Ohta, M. Hirano, H. Hosono, *Thin Solid Films* **2002**, *411*, 134.
[4] S.-A. Lee, J.-Y. Hwang, J.-P. Kim, S.-Y. Jeong, C.-R. Cho, *Appl. Phys. Lett.* **2006**, *89*, 182906.
[5] F. B. Zhang, K. Saito, T. Tanaka, M. Nishio, Q. X. Guo, *J. Cryst. Growth* **2014**, *387*, 96.
[6] K. D. Leedy, K. D. Chabak, V. Vasilyev, D. C. Look, J. J. Boeckl, J. F. Brown, S. E. Teflak, A. J. Green, N. A. Moser, A. Crespo, D. B. Thomson, R. C. Fitch, J. P. McCandless, G. H. Jessen, *Appl. Phys. Lett.* **2017**, *111*, 012103.
[7] X. H. Chen, S. Han, Y. M. Lu, P. J. Cao, W. J. Liu, Y. X. Zeng, F. Jia, W. Y. Xu, X. K. Liu, D. L. Zhu, *J. Alloys Compd.* **2018**, *747*, 869.
[8] H. Shen, K. Baskaran, Y. Yin, K. Tian, L. Duan, X. Zhao, A. Tiwari, *J. Alloys Compd.* **2020**, *822*, 153419.
[9] D. Splith, S. Müller, F. Schmidt, H. von Wenchstern, J. J. van Rensburg, W. E. Meyer, M. Grundmann, *Phys. Status Solidi A* **2014**, *211*, 40.
[10] D. Khan, D. Gajula, S. Okur, G. S. Tompa, G. Koley, *ECS J. Solid State Sci. Technol.* **2019**, *8*, Q106.
[11] C. Hou, R. A. Makin, K. R. York, S. M. Durbin, J. I. Scott, R. M. Gazoni, R. J. Reeves, M. W. Allen, *Appl. Phys. Lett.* **2019**, *114*, 235503.
[12] E. G. Villora, K. Shimamura, Y. Yoshikawa, T. Ujiie, K. Aoki, *Appl. Phys. Lett.* **2008**, *92*, 202120.
[13] F. Zhang, M. Arita, X. Wang, Z. Chen, K. Saito, T. Tanaka, M. Nishio, T. Motooka, Q. Guo, *Appl. Phys. Lett.* **2016**, *109*, 102105.
[14] S. Rafique, L. Han, A. T. Neal, S. Mou, M. J. Tadjer, R. H. Fench, H. Zhao, *Appl. Phys. Lett.* **2016**, *109*, 132103.
[15] Y. An, L. Dai, Y. Wu, B. Wu, Y. Zhao, T. Liu, H. Hao, Z. Li, G. Niu, J. Zhang, Z. Quan, S. Ding, *J. Adv. Dielectr.* **2019**, *9*, 1950032.
[16] K. Matsuzake, H. Hiramatsu, K. Nomura, H. Yanagi, T. Kamiya, M. Hirano, H. Hosons, *Thin Solid Films* **2006**, *496*, 37.
[17] J. Tauc, *Mater. Res. Bull.* **1968**, *3*, 37.
[18] R. Sharma, M. E. Law, C. Fares, M. Tadjer, F. Ren, A. Kuramata, S. J. Pearton, *AIP Adv.* **2019**, *9*, 855111.
[19] F. Zhang, K. Saito, T. Tanaka, M. Nishio, Q. Guo, *J. Mater. Sci: Mater. Electron.* **2015**, *26*, 9624.
[20] C. Hou, R. M. Gazoni, R. J. Reeves, M. W. Allen, *Appl. Phys. Lett.* **2019**, *114*, 033502.
[21] Q. He, W. Mu, H. Dong, S. Long, Z. Jia, H. Lv, Q. Liu, M. Tang, X. Tao, M. Liu, *Appl. Phys. Lett.* **2017**, *110*, 093503.
[22] D. Guo, Z. Wu, P. Li, Y. An, H. Liu, X. Guo, H. Yan, G. Wang, C. Sun, L. Li, W. Tang, *Opt. Mater. Express* **2014**, *4*, 1067.
[23] S. Nakagomi, T. Sakai, K. Kikuchi, Y. Kokubun, *Phys. Status Solidi A* **2019**, *216*, 1700796.

 © 2020 The Authors. Published by Wiley-VCH GmbH